High-Power Supercapacitor Electrodes from Single-Walled Carbon Nanohorn/Nanotube Composite

Ali Izadi-Najafabadi,[†] Takeo Yamada,[†] Don. N. Futaba,[†] Masako Yudasaka,[†] Hideyuki Takagi,[‡] Hiroaki Hatori,[‡] Sumio Iijima,[†] and Kenji Hata*[,†,§]

[†]Nanotube Research Center, Tsukuba, National Institute of Advanced Industrial Science and Technology (AIST), Tsukuba, 305-8565, Japan, [‡]Energy Technology Research Institute, National Institute of Advanced Industrial Science and Technology, AIST Tsukuba West, Tsukuba, 305-8569, Japan, and [§]Japan Science and Technology Agency (JST), Kawaguchi, 332-0012, Japan

ABSTRACT A novel composite is presented as a supercapacitor electrode with a high maximum power rating (990 kW/kg; 396 kW/l) exceeding power performances of other electrodes. The high-power capability of the electrode stemmed from its unique meso-macro pore structure engineered through the utilization of single-walled carbon nanotubes (20 wt %) as scaffolding for single-walled carbon nanohorns (80 wt %). The novel composite electrode also exhibited durable operation (6.5% decline in capacitance over 100 000 cycles) as a result of its monolithic chemical composition and mechanical stability. The novel composite electrode was benchmarked against another high-power electrode made from single-walled carbon nanotubes (Bucky paper electrode). While the composite electrode had a lower surface area compared to the Bucky paper electrode (280 *vs* 470 m^2/g from nitrogen adsorption), it had a higher meso-macro pore volume (2.6 *vs* 1.6 mL/g from mercury porosimetry) which enabled the composite electrode to retain more electrolyte, ensuring facile ion transport, hence achieving a higher maximum power rating (970 *vs* 400 kW/kg).

KEYWORDS: carbon nanohorns · carbon nanotubes · composite · electrodes · energy storage · supercapacitors

High-power electrical energy storage is critical to address emerging energy needs driven by new modes of production (*e.g.*, solar cells), distribution (*e.g.*, smart grid), and consumption (*e.g.*, electric vehicles) of electricity.[1] While batteries have been the primary choice for electrical energy storage, their reliance on chemical charge storage renders them unsuitable for high-power applications, as their charge/discharge speed is limited by chemical kinetics.[2] Electrochemical capacitors, also called supercapacitors, on the other hand primarily store energy physically (electrostatically) at the electrode/electrolyte interface and as such theoretically can operate at much faster rates albeit with reduced energy capacity compared to batteries.[3] Current commercial supercapacitors can operate at an order of magnitude higher power compared to batteries; however even such power levels are not sufficient to meet emerging needs.[4]

To achieve improved performance, the electrode needs a well-defined and tailored nanoscale structure. Nanomaterials, such as carbon nanotubes (CNTs), can have tailored and well-defined pore structures and thus pose the potential for superior ion accessibility and transport hence higher power performance.[5] This is in sharp contrast to conventionally used activated carbon (AC) materials which have a high surface area yet pose an intrinsically random winding pore structure limiting power performance. CNTs have been a particularly attractive alternative choice due to their well-defined nanostructure along with monolithic composition, chemical stability, and high electrical conductivity.[6]

For example, incorporation of multiwalled carbon nanotubes (MWNT) in AC electrodes has already shown increased power performance.[7−9] Furthermore, thin films of single-walled carbon nanotubes (SWNTs) (Bucky papers) have shown high enough electronic conductivity to be operational even without the need for current collectors.[10] Moreover, 4 V operation of SWNT electrodes has been achieved giving higher energy and power density compared to activated carbon electrodes.[11] Composite electrodes of carbon nanotubes with transition-metal oxides[12] or conducting polymers[13] have also achieved high capacitance performance at high discharge rates (for example, 100 F/g at 77 A/g), taking advantage of the conductive network of the carbon nanotubes and the pseudocapacitance properties of conducting polymers and transition-metal oxides.

Another form of carbon nanomaterials with monolithic chemical composition but different pore structure is single-walled carbon nanohorns (SWNH).[14] In contrast to the

*Address correspondence to kenji-hata@aist.go.jp.

Received for review July 23, 2010 and accepted December 26, 2010.

Published online January 06, 2011
10.1021/nn1017457

tubular structure of SWNTs, individual SWNHs have a conical structure with a base diameter of less than 5 nm and a length of less than 50 nm. SWNHs self-assemble to form Dahlia-like spheres with diameters below 100 nm, whereby the resulting spherical aggregates have minimum adhesion affinity for each other thus resulting in a powder.[15] SWNHs have a monolithic chemical composition as their synthesis process *via* laser ablation of graphite under vacuum is catalyst free.[14] Similar to CNTs, SWNHs have many promising applications,[16−19] and their potential as a supercapacitor electrode has been proven by initial research showing superior performance compared to activated carbon when operated in aqueous electrolyte.[20] As shown by the aforementioned examples, utilization of just a single type of nanomaterial, such as CNTs, can assist in engineering a well-defined, ordered pore structure. However, further improvement might be achieved by fabricating composite electrodes from nanomaterials having different shapes and length scales, whereby the pore structure could be tuned for both surface area and pore volume.

Here, we demonstrate a SWNH and SWNT composite electrode, with pore structure tailored for electrolyte retention, and thus delivering higher power compared to either SWNTs or SWNHs electrodes. The achieved power performance (maximum power rating approaching 1MW/kg when operated at 2.5 V) represents the highest value reported under similar device configuration. The monolithic chemical composition and mechanical stability of the electrode enabled excellent durability (6.5% decline over 100 000 cycles of operation). In this composite the long cylindrical SWNTs have been utilized as a binder and conducting agent for the spherical SWNH aggregates, resulting in a semidense (0.4 g/cm^3) electrode possessing sufficient pore volume for electrolyte retention and thus achieving higher power performance.

RESULTS AND DISCUSSION

Utilization of composites as electrodes for supercapacitors in itself is not a new concept. For example, the AC electrode widely used is, in fact, a composite compromised of AC powder mixed with a conducting agent, *e.g.*, carbon black, and a binding agent, *e.g.*, PTFE. Composites of SWNTs and transition-metal oxides have also been explored showing promising high-power performance.[21] In constructing our novel composite electrode, a new approach was adopted whereby the constituents of the composite have overlapping multifunctional roles. The SWNTs act as both a conductivity enhancer and a binding agent providing mechanical stability, while their high surface area also provides capacitance. The SWNH particles act as the capacitive interface as well as a crucial component to tailor the electrode pore structure.

Specifically, to achieve a chemically pure, highly conductive and mechanically stable SWNH/SWNT composite, SWNTs grown using water-assisted chemical vapor deposition (supergrowth)[22] were utilized due to their chemical purity,[23] limited bundling, high surface area,[24] and mm-scale tube length.[25] The composite was assembled by first mixing SWNH particles (80 wt %) with SWNTs (20 wt %) in dimethyl formamide (DMF), as shown in Figure 1a; with the ratios chosen on the basis of those commonly used in preparation of AC electrodes. After sonication at moderate power in DMF, the well-dispersed suspension of SWNT and SWNH particles was poured into a glass dish resting on a hot plate placed on a flat surface under a fume hood. Upon evaporation of DMF a self-supporting film (Figure 1b and c) easily removable from the glass dish was formed (density of 0.4 g/cc, DC conductivity of 20 S/cm). As shown in the Supporting Information, thermogravimetric analysis of the as-prepared composite *via* heating at a rate of 2 °C/min under dry air flow showed only one peak suggesting a monolithic chemical composition. For comparison SWNT Bucky papers (density of 0.6 g/cc, DC conductivity of 70 S/cm) were made in a similar manner to the composite albeit using only SWNTs. Scanning electron microscopy (SEM) of the composite revealed the role of SWNTs in providing adhesion and interconnection for the SWNH particles (Figure 1g). Comparison of the SEM micrographs of SWNH/SWNT composite with the SWNT Bucky paper (Figure 1h) revealed the unique role of the ball-like SWNH aggregates as spacers leading to a meso-macro pore structure, which accounts for the high-power performance of the composite electrode as discussed later.

While the ball-like SWNH aggregates were critical in achieving the desired pore structure, the closed structure of the aggregate rendered the interstitial void volume of the SWNH particles inaccessible thus potentially reducing capacitance. To overcome this issue, hole opening,[20,24] *via* a previously established oxidation process for SWNTs and SWNHs, was applied to the composite. To ensure a fair comparison between the as-prepared composite, the oxidized composite and the SWNT Bucky paper, electrodes with the same area (6 × 6 mm) and similar weight were cut from the original films using a laser marker (Keyence MD-V). Supercapacitors were then assembled by stacking a separator in between two identical electrodes supported with platinum mesh current collectors with 1 M Et_4NBF_4/propylene carbonate as the electrolyte (Tomiyama Pure Chemical) in a screwed cell.

First the operating voltage range of the electrodes was determined by cyclical voltammetry (CV) (Figure 2a). All electrodes exhibited stable operation up to 2.5 V, which agreed with previous report on SWNHs.[21] While supergrowth SWNTs are operational up to 4 V in the same electrolyte media,[14] the CV profiles of the asprepared composite and the oxidized composite exhibited a peaked shape starting at 2 V, which suggested their operating voltage range could not be extended

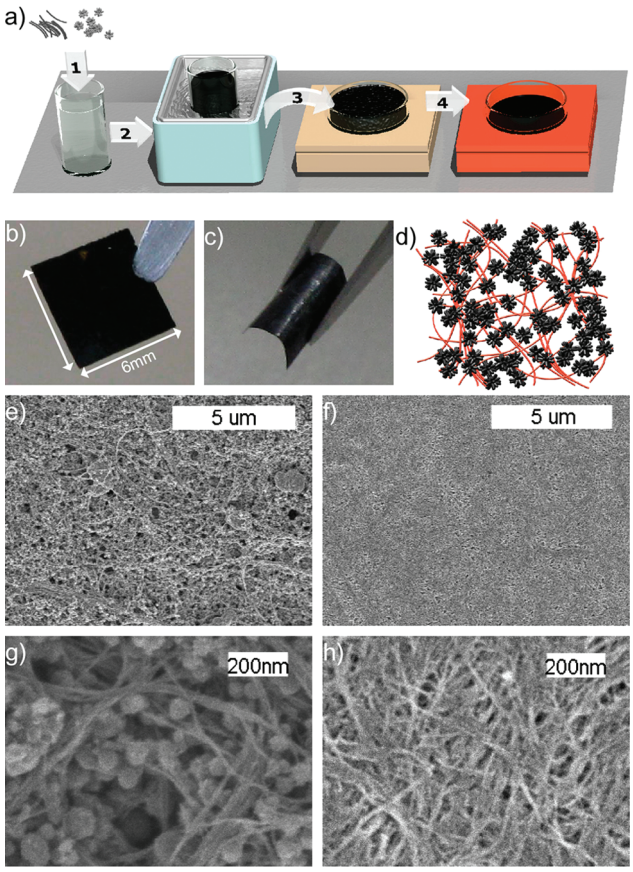

Figure 1. SWNH/SWNT composite. (a) Fabrication process: (1) 8 mg of SWNH powder and 2 mg of supergrowth SWNT are mixed with 10 mL of DMF. (2) A suspension is formed after 24 hrs of sonication at moderate power (40 W). (3) The resulting suspension is then poured into a dish (3 cm diameter) resting on a hot plate (set to 100 °C) placed on a flat surface inside a fume hood under negative pressure. (4) Upon solvent evaporation (after ~8hrs), a self-supporting film easily removable from the dish is formed. (b) Image of a typical SWNH/SWNT composite electrode. (c) Image of the same electrode bent to show its self-supporting capability. (d) Schematic depicting the role of SWNTs as scaffolding for SWNH particles. (e) SEM micrograph of the SWNH/SWNT composite. (f) SEM micrograph of the SWNT Bucky paper. (g) Higher magnification SEM micrograph of SWNH/SWNT composite showing the SWNTs connecting the SWNH particles. (h) Higher magnification SEM micrograph of the SWNT Bucky paper showing smaller pore volume compared to the SWNH/SWNT composite.

far beyond 2.5 V without initiating parasitic reactions. As such, the operating voltage range of the composite electrodes was similar to that of conventional AC electrodes. In the case of AC electrodes the limited operating voltage range is primarily due to presence of chemical impurities and surface functional groups. As the composite electrode is chemically pure, the limited operating voltage range may be attributed to presence of dangling bonds along the edges of the SWNH particles.[26] We believe that passivation of these dangling bonds would enable a wider operating voltage range. The lower cell voltage limit of 2.5 V for the SWNH/SWNT composite results in lowering the energy density of these electrodes by at least 2.5 times compared to the supergrowth SWNT electrodes[14] just on the basis of cell voltage difference alone ($E \sim 1/2CV^2$).

Close examination of the CV profiles also demonstrated the difference in the underlying capacitance mechanism of the electrodes. At 0 V DC, capacitance (as indicated by the discharge CV current) was primarily due to double-layer charging. Here, the oxidized composite electrode exhibited the highest capacitance in agreement with its higher surface area as later confirmed *via* nitrogen adsorption isotherms. As the voltage was increased, the capacitance of the composite electrodes did not appear to significantly change. In contrast, the SWNT Bucky paper showed an increase in capacitance as a function of voltage due to electrochemical doping.[27,28]

To quantitatively evaluate the performance of the electrodes, galvanostatic (constant current) discharges were measured from 0.1 to 50 A/g. The capacitance (Figure 2b) and the internal resistance values were then determined from the slope and the initial voltage drop (Figure 2c) of the discharge curves, respectively. First the capacitance results are discussed. The composite electrodes exhibited lower decline in capacitance as the discharge rate was increased compared to the Bucky paper electrode, suggesting superior ion transport properties. Specifically, the as-prepared composite exhibited a capacitance of 46 F/g at 0.1 A/g and a capacitance of 36 F/g at 50 A/g (21% decline), while the

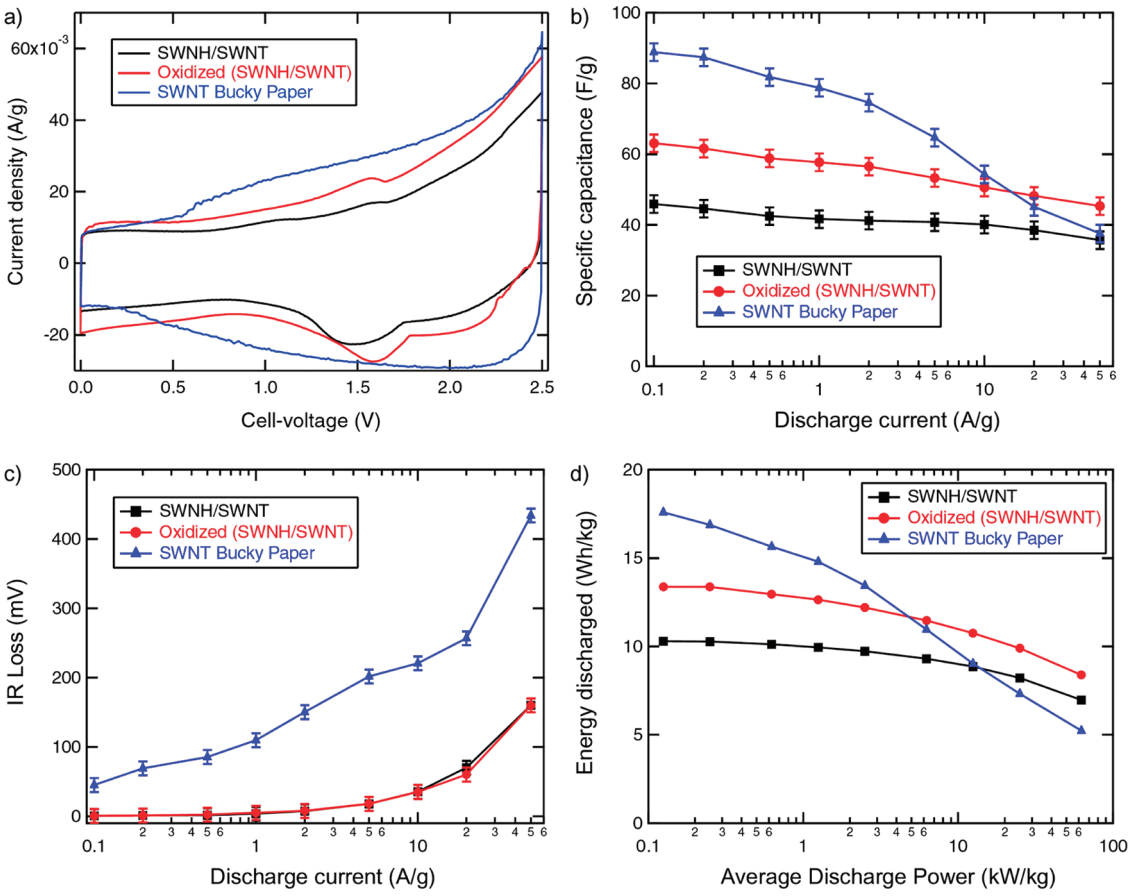

Figure 2. Electrochemical performance of SWNH/SWNT composite and SWNT Bucky paper electrodes. (a) CV of as-prepared composite of SWNH/SWNT (black), oxidized composite of SWNH/SWNT (red), and SWNT Bucky paper (blue) measured at 1 mV/s. All electrodes appear to be operational up to 2.5 V, with the SWNT Bucky paper showing an overall higher capacitance as evidenced by the larger discharge (negative) current. (b) Specific capacitance of as-prepared composite of SWNH/SWNT (black), oxidized composite of SWNH/SWNT (red), and SWNT Bucky paper (blue) determined from the slope of constant current (galvanostatic) discharge curves. While at lower discharge rates the SWNT Bucky paper shows higher capacitance, at higher currents its performance declines to the same level as that of the as-prepared composite. (c) IR loss of as-prepared composite of SWNH/SWNT (black), oxidized composite of SWNH/SWNT (red), and SWNT Bucky paper (blue). At any discharge rate the composite electrodes have a lower IR loss compared to the SWNT Bucky paper electrode. (d) Ragone plot of the overall performance of all electrodes.

oxidized composite exhibited a capacitance of 63 F/g at 0.1 A/g and a capacitance of 45 F/g at 50 A/g (29% decline), whereas the SWNT Bucky paper exhibited a capacitance of 89 F/g at 0.1 A/g and a capacitance of 37 F/g at 50 A/g (58% decline).

Comparison of the IR loss values (Figure 2c) further confirmed the superior transport properties of the composite. The IR loss values of the SWNH/SWNT composite electrodes were significantly lower than the Bucky paper at all discharge rates, which was surprising considering the lower DC electronic conductivity of the SWNH/SWNT composite electrodes (20 S/cm) compared to the Bucky Paper (70 S/cm). This seemingly contradictory result could be attributed to the meso-macro pore structure of the SWNH/SWNT composite electrodes resulting in enhanced retention of electrolyte thus enabling faster ion access compared to the SWNT Bucky paper, as confirmed later *via* mercury porosimetry. It is worth to note that the IR loss values of the SWNT Bucky paper were already a significant improvement (more than five times less under similar configuration) over AC electrodes.[11,24] Based on the cell internal resistance values determined from the IR loss values, the maximum power rating for the as-prepared composite was 970 kW/kg, while the oxidized composite was 990 kW/kg and the Bucky paper 400 kW/kg. For AC electrodes under similar device geometry, the estimated maximum power rating would be only 80 kW/kg,[11,24] *i.e.*, more than 10 times less than the SWNH/SWNT composite electrodes.

The overall operational characteristics of the electrodes were demonstrated by the Ragone plot in Figure 2d, based on the energy discharged ($E = \int IV(t)dt$) at different average discharge powers ($P_{Average} = IV/2$). The superior power performance of the SWNH/SWNT composite electrodes was highlighted by their ability to discharge more energy compared to the Bucky paper electrode at the higher end of the power spectrum. Specifically starting from the average discharge power of 6.25 kW/kg (*i.e.*, discharging at 5 A/g),

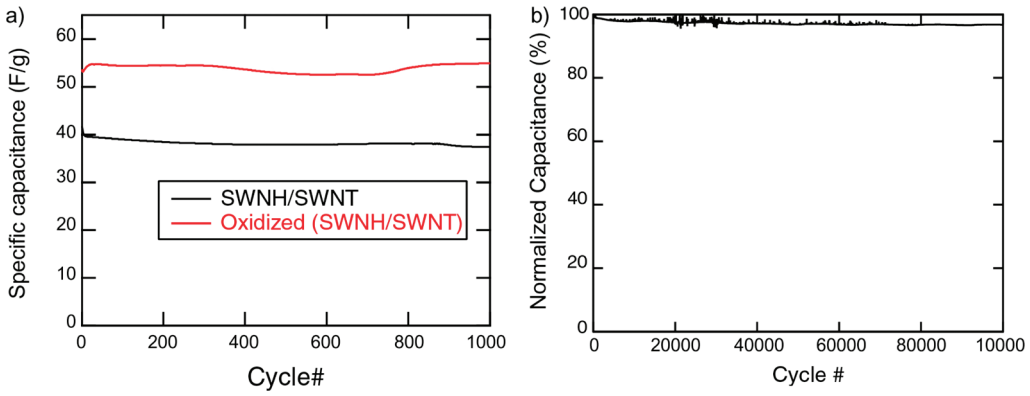

Figure 3. Dynamic lifetime of the composite electrodes. (a) Over 1000 cycles of charge/discharge at 1A/g, only minor degradation in performance is observed. (b) Durability testing over 100 000 cycles of charge/discharge at 10A/g indicates that after minor degradation in performance during the first few thousand cycles, the performance of the electrodes reaches a stable plateau.

the energy discharged by the oxidized SWNH/SWNT composite electrodes was higher than that of the Bucky paper electrode. In the case of the as-prepared composite, more energy could be discharged compared to the Bucky paper electrode starting from 12.5 kW/kg (*i.e.*, discharging at 10 A/g).

While these results establish the superior power capability of the SWNH/SWNT composite electrodes, the durability of the composite electrodes over repeated operations needed examination. To this end, the as-prepared and oxidized composites were subjected to 1000 cycles of full-depth charge/discharge at 1 A/g. As shown in Figure 3a, the capacitance of the electrodes barely changed over the continuous operation with the as-prepared composite, declining by only 6%, and the oxidized composite slightly declining in performance midcycle and subsequently recovering. Durability testing of the as-prepared composite at higher rates (10 A/g) for a longer duration (100 000 cycles) showed that the majority of variability and decline in capacitance occurred during the initial few thousand cycles (Figure 3b). From 50 000 to 100 000 cycles, the decline in performance was only 0.2%. The durability of the composite electrodes could be attributed to their chemical purity and mechanical stability courtesy of the SWNTs providing good adhesion for the SWNH particles.

To investigate the underlying cause of the superior power performance of the SWNH/SWNT composite electrodes, the pore structure of the electrodes was examined *via* nitrogen adsorption/desorption and mercury porosimetry (Figure 4a and c, respectively). The nitrogen adsorption isotherm of the as-prepared composite (black) showed a very similar profile to that of as-grown SWNH powder (green), and Brunauer–Emmett–Teller (BET) analysis[29] of these isotherms results in similar specific surface area values: 280 m^2/g for the as-prepared composite and 350 m^2/g for the as-grown SWNH powder. The similar specific surface areas (280 *vs* 350 m^2/g) accounted for the similar capacitance values (46 *vs* 43 F/g) observed for the as-prepared SWNT/SWNH composite and the as-grown SWNH electrode reported elsewhere,[20] respectively. The low surface area of SWNH powder, and the resultant SWNH/SWNT composite, was attributed to individual SWNHs forming aggregates (the ball-like structures apparent in the SEM image of Figure 1g), whereby the interstitial pore volume of the aggregates were inaccessible. BET analysis of the nitrogen adsorption profile of the SWNT Bucky paper resulted in a specific surface area of 470 m^2/g, which was lower than that of the surface area of as-grown supergrowth SWNTs (>1100 m^2/g),[23] suggesting the overlapping of SWNTs observable in the SEM micrograph of the SWNT Bucky paper (Figure 1h) had reduced the accessible surface area. For the oxidized composite (red), the nitrogen volume absorbed was significantly higher, and its BET specific surface area was 1430 m^2/g, *i.e.*, more than five times that of the as-prepared composite, suggesting access to the interstitial pore volume of the SWNH aggregates. However, the oxidized composite exhibited only a modest gain (37%) in capacitance compared to the as-prepared SWNH/SWNT composite electrode's capacitance. To investigate this disparity, Barret–Joyner–Halenda (BJH) analysis[30] was applied to the adsorption isotherms (Figure 4b). From BJH analysis, the majority of the gain in surface area is attributed to hole openings within the micropore range (<2 nm according to IUPAC classification),[31] which are inaccessible to the solvated ions of the organic electrolyte used here. This result is in agreement with previous reports on electrodes made from oxidized SWNHs.[20]

While the nitrogen adsorption measurement was insightful in determining specific surface areas and pore structures within the micro-meso pore range, the macroporosity of interest for electrolyte retention is better examined using mercury porosimetry[32] (Figure 4c and d), as the macropore range (>50 nm) measurement based on gas adsorption is unreliable.[33] As shown in Figure 4c, the total mercury intrusion volume

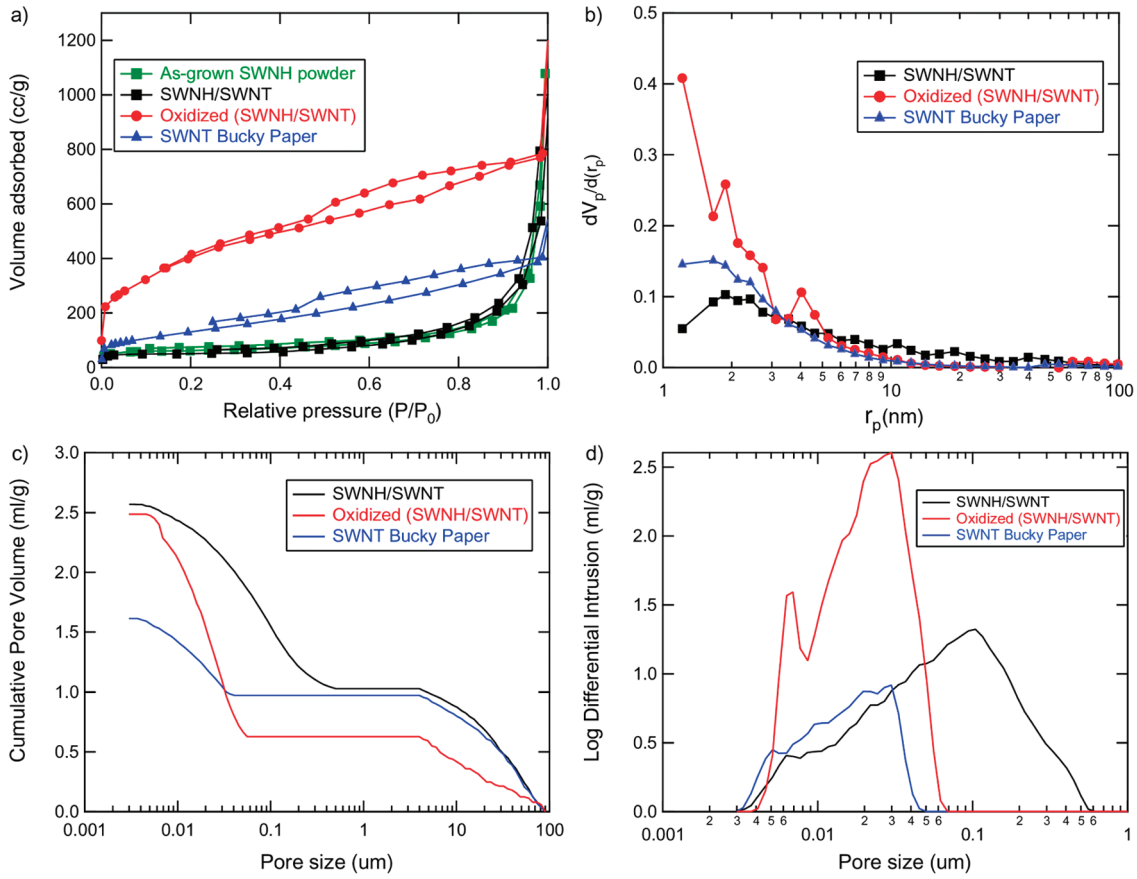

Figure 4. Specific surface area and pore characterization of the composites. (a) Nitrogen adsorption/desorption isotherms at 77K for as-grown SWNH powder (green), composite of SWNH/SWNT (black), oxidized composite SWNH/SWNT composite (red), and SWNT Bucky paper (blue). The as-prepared composite appears to have the same surface area as that of as-grown SWNH powder, whereas the oxidized composite exhibits five times the surface area of the as-prepared composite. (b) BJH plot depicting the pore distribution of the as-prepared composite (black), the oxidized composite (red), and SWNT Bucky paper (blue). The surface area gain of the oxidized composite is attributed to micropores inaccessible to the organic electrolyte. (c) Mercury cumulative intrusion volume normalized by electrode weight. The composite samples absorb a higher volume of mercury. (d) Log differential of the cumulative intrusion profile indicating the pore size distribution. The composite samples have a pore distribution centered at a wider pore diameter. The difference in the pore distribution indicated by mercury porosimetry and nitrogen adsorption is partly due to intrinsic differences in the underlying measurement phenomena and to presence of wide void pockets with narrow entrances (and *vice versa*).

(normalized by electrode weight) was the highest for the as-prepared composite (2.6 mL/g), followed closely by the oxidized composite (2.5 mL/g), whereas the SWNT Bucky paper showed a significantly lower intrusion volume (1.6 mL/g), thus confirming the electrolyte uptake of the SWNH/SWNT composite electrodes was higher than that of the SWNT Bucky paper electrode.

The electrolyte volume uptake of the electrode is critical in terms of power performance. During charging, a high concentration of ions has to be amassed at the electrode surface, as such the ionic concentration of the electrolyte within the void volume of the electrode would be lowered. Given sufficient electrolyte within the electrode, the change in ionic concentration would not be substantial, and there would be sufficient ions to facilitate conduction during charge/discharge. However, if there is insufficient electrolyte within the electrode, charging would result in depletion of ions within the electrode thus resulting in a lower power.

Using the specific capacitance of the electrodes (at 0.1A/g) and the basic capacitor model ($Q = CV$), the charge concentration required for charging to 2.5 V was estimated as: 56 C/g for the as-prepared composite, 79 C/g for the oxidized composite, and 111 C/g for the Bucky paper. The electrolyte used had a concentration of 1 mol, *i.e.*, 1 ml of the electrolyte would correspond to an ionic charge of 96 C. Assuming the electrolyte volume uptake of the electrodes was similar to their mercury intrusion volumes, the estimated charge concentration within each electrode would be: 240 C/g for the as-prepared composite, 231 C/g for the oxidized composite, and 154 C/g for the Bucky paper. Comparing the ionic charge concentration available within the electrode and the charge concentration required at the double-layer during charging, it is clear that in the case of the as-prepared composite, while the ionic concentration within the electrode would be reduced (~27% reduction), there would still be sufficient amount of ions to maintain conduction.

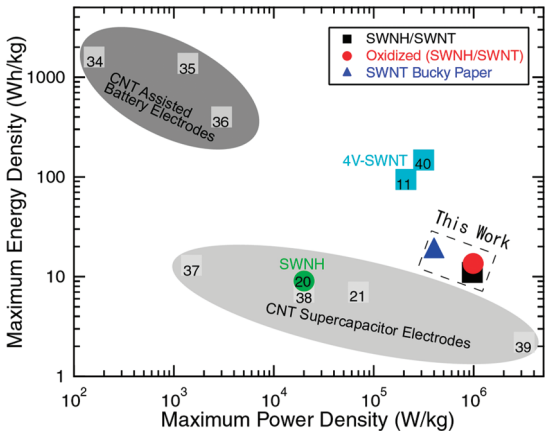

Figure 5. Electrodes' performance comparison. The power performance of the SWNH/SWNT composite electrode surpasses other nanocarbon electrodes.

In the case of the oxidized composite the situation was slightly worse (~34% reduction). For the Bucky paper, significant reduction in the charge concentration (~60%) would hinder transport as less ions would be available within the pore volume of the electrode. In contrast, the ability of the composite electrodes to retain large amounts of electrolytes, even at high discharge rates, would provide for sufficient ions within the electrode itself to facilitate charge/discharge, as was observed in the capacitance and IR loss results previously discussed. While the preceding analysis should be considered qualitative due to the overly simplified model used, it illustrates the importance of not only considering electrode surface area but also the electrode pore volume available for electrolyte retention.

The maximum power performance of the composite and Bucky paper electrodes were compared to other nanocarbon electrodes, as shown in Figure 5; this is a provisional comparison as the testing geometries were not the same for all the reference data. The maximum power rating of the SWNH/SWNT composite electrode (990 kW/kg) was almost twenty times higher than the estimated maximum power performance (~50 kW/kg) of the only previous report on SWNH electrodes,[21] and more than twice that of the SWNT Bucky paper (400 kW/kg) examined here. Comparison of the performance of the composite electrodes with other nanocarbon electrodes (Figure 5) showed that while the composite electrodes have been operated only at 2.5 V, their maximum power rating still surpassed other nanocarbon electrodes.

The only electrode (nanocarbon based or otherwise) reported having a higher maximum power (3.2 MW/kg, 16 kW/l *vs* 0.99 MW/kg, 396 kW/l for the composite electrodes) was composed of a sparse MWNT forest electrode (density of 0.005 g/cm^3). Sparse CNT forest electrodes naturally have higher power performance as essentially individual CNTs within the forest are immersed in an almost infinite sea of electrolyte, *i.e.*, infinite supply of ions. Here, our composite material has achieved a similar power performance, by tailoring the pore structure to optimize electrolyte retention yet having a density eighty times that of the sparse CNT forest.

In conclusion we have fabricated a new composite from SWNHs and SWNTs possessing a meso-micro pore structure. The composite utilized as a supercapacitor electrode achieves a maximum power rating (1 MW/kg) surpassing other electrodes. The high-power performance can be traced to facile ion transport as a result of the semidense composite's ability to hold sufficient electrolytes within its void volume.

EXPERIMENTAL METHODS

Hole Opening *via* Oxidation. The opening process was carried out by using a muffle furnace (KDF P-70) at a ramping rate of 1 °C/min heated to 525 °C under dry air flow (2000 sccm). The cooling cycle was not controlled.

Surface Area Measurement. Nitrogen adsorption and desorption isotherms at 77 K were measured using a BEL (Japan) Inc. Belsorp-28SA surface area and pore size analysis system. All samples were pretreated under vacuum at 150 °C for 12 h prior to measurement.

Mercury Porosimetry. Mercury porosimetry was carried out using a Shimadzu Micromeritics Autopore IV 9500 automated mercury porosimeter. All calculations assume a contact angle of 130° and mercury surface tension of 485 dyn/cm. Prior to measurement, samples were pretreated similar to the samples used for nitrogen adsorption measurement.

Supercapacitor Assembly and Testing. Excluding the electrolyte, all active components of the supercapacitors: electrodes, separators, and current collectors were vacuum dried at 150 °C for at least 8 h prior to device assembly. The cells were assembled in a dry argon environment, using platinum mesh (100 mesh, Nilaco Corp.) current collectors, a porous proprietary cellulous-based separator (40 μm thickness, density *ca.* 0.6 g/cm^3), and 1 M Et4NBF4/propylene carbonate as electrolyte (Tomiyama Pure Chemical). Electrochemical characteristics were obtained using VMP3 galvanostat/potentiostat/frequency response analyzer (Princeton Applied Research). The maximum power rating[3,4] was calculated based on the internal resistance (R_S) values determined from a linear fit[11] to the IR loss values in Figure 2C. Linear fit model for IR_{loss}: $IR_{loss} = a + b*I$, where a represents the difference in the 2.5 V applied and the charged potential of the capacitor and b represents double the value of the internal resistance (R_S) and I is discharge − current.

$$P_{max} = \frac{V_{OCV}^2}{4R_S} = \frac{(2.5-a)^2}{2b}$$

By definition specific capacitance refers to capacitance of a single electrode.[2] All other values (current, energy, and maximum power densities) were normalized with respect to the combined weight of both electrodes.

Acknowledgment. We wish to thank Ms. Megumi Kikuchi for assistance with nitrogen adsorption measurements and Dr. Tatsuo Toida for assistance with schematic preparation. Partial support by Core Research for Evolution Science and Technology

(CREST) program of Japan Science and Technology Agency (JST) is acknowledged.

Supporting Information Available: Galvanostatic discharge profiles, impedance spectroscopy results, additional dynamic lifetime measurement profiles, and thermogravimetric analysis. This material is available free of charge *via* the Internet at http://pubs.acs.org.

REFERENCES AND NOTES

1. *Basic Research Needs for Electrical Energy Storage*. Report of the Basic Energy Workshop on Electrical Energy Storage; Department of Energy: Washington, DC, 2007; http://www.sc.doe.gov/bes/reports/files/EES_rpt.pdf
2. Conway, B. E. In *Electrochemical Supercapacitors: Scientific Fundamentals and Technological Applications*; Kluwer Academic/Plenum Publishers: New York, 1999.
3. Kötz, R.; Carlen, M. Principles and Applications of Electrochemical Capacitors. *Electrochim. Acta* **2000,** *45*, 2483–2498.
4. Burke, A. Ultracapacitors: Why, How, and Where Is the Technology. *J. Power Sources* **2000,** *91*, 37–50.
5. Simon, P.; Gogotsi, Y. Materials for Electrochemical Capacitors. *Nat. Mater.* **2008,** *7*, 845–854.
6. Niu, C.; Sichel, E. K.; Hoch, R.; Moy, D.; Tennent, H. High Power Electrochemical Capacitors Based on Carbon Nanotube Electrodes. *Appl. Phys. Lett.* **1997,** *70*, 1480–1482.
7. Portet, C.; Taberna, P. L.; Simon, P.; Flahaut, E.; Laberty-Robert, C. High Power Density Electrodes for Carbon Supercapacitor Applications. *Electrochim. Acta* **2005,** *50*, 4174–4181.
8. Show, Y.; Imaizumi, K. Electric Double Layer Capacitor with Low Series Resistance Fabricated by Carbon Nanotube Addition. *Diamond Relat. Mater.* **2007,** *16*, 1154–1158.
9. Huang, C.-W.; Chuang, C.-M.; Ting, J.-M.; Teng, H. Significantly Enhanced Charge Conduction in Electric Double Layer Capacitors Using Carbon Nanotube-Grafted Activated Carbon Electrodes. *J. Power Sources* **2008,** *183*, 406–410.
10. Kaempgen, M.; Chan, C. K.; Ma, J.; Cui, Y.; Gruner, G. Printable Thin Film Supercapacitors Using Single-Walled Carbon Nanotubes. *Nano Lett.* **2009,** *9*, 1872–1876.
11. Izadi-Najafabadi, A.; Yasuda, S.; Kobashi, K.; Yamada, T.; Futaba, D. N.; Hatori, H.; Yumura, M.; Iijima, S.; Hata, K. Extracting the Full Potential of Single-Walled Carbon Nanotubes as Durable Supercapacitor Electrodes Operable at 4 V with High Power and Energy Density. *Adv. Mater.* **2010**, *22*, E235−E241.
12. Hou, Y.; Cheng, Y.; Hobson, T.; Liu, J. Design and Synthesis of Hierarchical MnO_2 Nanospheres/Carbon Nanotubes/Conducting Polymer Ternary Composite for High Performance Electrochemical Electrodes. *Nano Lett.* **2010,** *10*, 2727–2733.
13. Khomenko, V.; Frackowiak, E.; Béguin, F. Determination of the Specific Capacitance of Conducting Polymer/Nanotubes Composite Electrodes Using Different Cell Configurations. *Electrochim. Acta* **2005,** *50*, 2499–2506.
14. Iijima, S.; Yudasaka, M.; Yamada, R.; Bandow, S.; Suenaga, K.; Kokai, F.; Takahashi, K. Nano-Aggregates of Single-Walled Graphitic Carbon Nano-Horns. *Chem. Phys. Lett.* **1999,** *309*, 165–170.
15. Murata, K.; Kaneko, K.; Kokai, F.; Takahashi, K.; Yudasaka, M.; Iijima, S. Pore Structure of Single-Wall Carbon Nanohorn Aggregates. *Chem. Phys. Lett.* **2000,** *331*, 14–20.
16. Murata, K.; Hashimoto, A.; Yudasaka, M.; Kasuya, D.; Kaneko, K.; Iijima, S. The Use of Charge Transfer to Enhance the Methane-Storage Capacity of Single-Walled, Nanostructured Carbon. *Adv. Mater.* **2004,** *16*, 1520–1522.
17. Zhang, M.; Yudasaka, M.; Ajima, K.; Miyawaki, J.; Iijima, S. Light-Assisted Oxidation of Single-Wall Carbon Nanohorns for Abundant Creation of Oxygenated Groups That Enable Chemical Modifications with Proteins To Enhance Biocompatibility. *ACS Nano* **2007,** *1*, 265–272.
18. Zhu, S.; Fan, L.; Liu, X.; Shi, L.; Li, H.; Han, S.; Xu, G. Determination of Concentrated Hydrogen Peroxide at Single-Walled Carbon Nanohorn Paste Electrode. *Electrochem. Commun.* **2008,** *10*, 695–698.
19. Wen, D.; Deng, L.; Zhou, M.; Guo, S.; Shang, L.; Xu, G.; Dong, S. A Biofuel Cell with a Single-Walled Carbon Nanohorn-Based Bioanode Operating at Physiological Condition. *Biosens. Bioelectron.* **2010,** *25*, 1544–1547.
20. Yang, C.-M.; Kim, Y.-J.; Endo, M.; Kanoh, H.; Yudasaka, M.; Iijima, S.; Kaneko, K. Nanowindow-Regulated Specific Capacitance of Supercapacitor Electrodes of Single-Wall Carbon Nanohorns. *J. Am. Chem. Soc.* **2007,** *129*, 20–21.
21. Zhang, H.; Cao, G.; Wang, Z.; Yang, Y.; Shi, Z.; Gu, Z. Growth of Manganese Oxide Nanoflowers on Vertically-Aligned Carbon Nanotube Arrays for High-Rate Electrochemical Capacitive Energy Storage. *Nano Lett.* **2008,** *8*, 2664–2668.
22. Hata, K.; Futaba, D. N.; Mizuno, K.; Namai, T.; Yumura, M.; Iijima, S. Water-Assisted Highly Efficient Synthesis of Impurity-Free Single-Walled Carbon Nanotubes. *Science* **2004,** *306*, 1362–1364.
23. Yasuda, S.; Hiraoka, T.; Futaba, D. N.; Yamada, T.; Yumura, M.; Hata, K. Existence and Kinetics of Graphitic Carbonaceous Impurities in Carbon Nanotube Forests to Assess the Absolute Purity. *Nano Lett.* **2009,** *9*, 769–773.
24. Hiraoka, T.; Izadi-Najafabadi, A.; Yamada, T.; Futaba, D. N.; Yasuda, S.; Tanaike, O.; Hatori, H.; Yumura, M.; Iijima, S.; Hata, K. Compact and Light Supercapacitor Electrodes from a Surface-Only Solid by Opened Carbon Nanotubes with 2200 m^2g^{-1} Surface Area. *Adv. Funct. Mater.* **2010,** *20*, 422–428.
25. Yasuda, S.; Futaba, D. N.; Yamada, T.; Satou, J.; Shibuya, A.; Takai, H.; Arakawa, K.; Yumura, M.; Hata, K. Improved and Large Area Single-Walled Carbon Nanotube Forest Growth by Controlling the Gas Flow Direction. *ACS Nano* **2009,** *3*, 4164–4170.
26. Utsumi, S.; Honda, H; Hattori, Y.; Kanoh, H.; Takahashi, K.; Sakai, H.; Abe, M.; Yudasaka, M.; Iijima, S.; Kaneko, K. Direct Evidence on C-C Single Bonding in Single-Wall Carbon Nanohorn Aggregates. *J. Phys. Chem. C* **2007,** *111*, 5572–5575.
27. Hahn, M.; Baertschi, M.; Barbieri, O.; Sauter, J.-C.; Kötz, R.; Gallay, R. Interfacial Capacitance and Electronic Conductance of Activated Carbon Double-Layer Electrodes. *Electrochem. Solid-State Lett.* **2004,** *7*, A33–A36.
28. Kimizuka, O.; Tanaike, O.; Yamashita, J.; Hiraoka, T.; Futaba, D. N.; Hata, K.; Machida, K.; Suematsu, S.; Tamamitsu, K.; Saeki, S.; *et al.* Electrochemical Doping of Pure Single-Walled Carbon Nanotubes Used as Supercapacitor Electrodes. *Carbon* **2008,** *46*, 1999–2001.
29. Brunauer, S.; Emmett, P. H.; Teller, E. Adsorption of Gases in Multimolecular Layers. *J. Am. Chem. Soc.* **1938,** *60*, 309–319.
30. Barret, E. P.; Joyner, L. G.; Halenda, P. H. The Determination of Pore Volume and Area Distributions in Porous Substances. I. Computations from Nitrogen Isotherms. *J. Am. Chem. Soc.* **1951,** *73*, 373–380.
31. International Union of Pure and Applied Chemistry Physical Chemistry Division Commission on Colloid and Surface Chemistry, Subcommittee on Characterization of Porous Solids: "Recommendations for the characterization of porous solids (Technical Report)". *Pure Appl. Chem.* 1994, *66*, 1739-1758.
32. Washburn, E. W. Note on a Method of Determining the Distribution of Pore Sizes in a Porous Material. *Proc. Natl. Acad. Sci. U.S.A.* **1921,** *7*, 115–116.
33. Gregg, S. J. Sing, K. S. W. In *Adsorption, Surface Area and Porosity*; Kluwer Academic Press: New York, 1982.
34. Reddy, A. L. M.; Shaijumon, M. M.; Gowda, S. R.; Ajayan, P. M. Coaxial MnO2/Carbon Nanotube Array Electrodes for High-Performance Lithium Batteries. *Nano Lett.* **2009,** *9*, 1002–1006.
35. Masarapu, C.; Subramanian, V.; Zhu, H.; Wei, B. Long-Cycle Electrochemical Behavior of Multiwall Carbon Nanotubes Synthesized on Stainless Steel in Li Ion Batteries. *Adv. Funct. Mater.* **2009,** *19*, 1008–1014.
36. Lee, Y. J.; Yi, H.; Kim, W.-J.; Kang, K.; Yun, D. S.; Strano, M. S.; Ceder, G.; Belcher, A. M. Fabricating Genetically Engineered

High-Power Lithium-Ion Batteries Using Multiple Virus Genes. *Science* **2009,** *324*, 1051–1055.
37. Pushparaj, V. L.; Shaijumon, M. M.; Kumar, A.; Murugesan, S.; Ci, L.; Vajtai, R.; Linhardt, R. J.; Nalamasu, O.; Ajayan, P. M. Flexible energy storage devices based on nanocomposite paper. *Proc. Natl. Acad. Sci. U.S.A.* **2007,** *104*, 13574–13577.
38. An, K. H.; Kim, W. S.; Park, Y. S.; Moon, J.-M.; Bae, D. J.; Lim, S. C.; Lee, Y. S.; Lee, Y. H. Electrochemical Properties of High-Power Supercapacitors Using Single-Walled Carbon Nanotube Electrodes. *Adv. Funct. Mater.* **2001,** *11*, 387–392.
39. Honda, Y.; Haramoto, T.; Takeshige, M.; Shiozaki, H.; Kitamura, T.; Ishikawa, M. Aligned MWCNT Sheet Electrodes Prepared by Transfer Methodology Providing High-Power Capacitor Performance. *Electrochem. Solid-State Lett.* **2007,** *10*, A106–A110.
40. Lu, W.; Qu, L.; Henry, K.; Dai, L. High Performance Electrochemical Capacitors from Aligned Carbon Nanotube Electrodes and Ionic Liquid Electrolytes. *J. Power Sources* **2009,** *189*, 1270–1277.